Published in final edited form as:
Immunotherapy. 2012 February ; 4(2): 151–161. doi:10.2217/imt.11.163.

Modulating intestinal immune responses by lipoteichoic acid-deficient *Lactobacillus acidophilus*

Mohammad W Khan[1], **Mojgan Zadeh**[2], **Praveen Bere**[2], **Elias Gounaris**[1], **Jennifer Owen**[2], **Todd Klaenhammer**[3], and **Mansour Mohamadzadeh**[2,*]

[1]Northwestern University, Feinberg School of Medicine, Chicago, IL 60611, USA

[2]Department of Infectious Diseases & Pathology and Emerging Pathogens Institute, PO Box 110880, 2015 SW 16th Ave, Gainesville, FL 32611-0882, USA

[3]Department of Food, Bioprocessing & Nutrition Sciences, NC State University, Raleigh, NC, USA

Abstract

Aim—To investigate the mechanism(s) by which the intestinal commensal microbe *Lactobacillus acidophilus* can affect host immunity, we studied the role of a component of the cell wall, lipoteichoic acid, in colitis.

Materials & methods—Colitis was induced by the intraperitoneal injection of pathogenic $CD4^+CD25^-CD45RB^{hi}$ T cells into *Rag1*$^{-/-}$ mice. The parental strain, NCK56, or the lipoteichoic acid-deficient strain, NCK2025, was then administered orally. Fluorescent microscopy was employed to examine resulting cell populations and their cytokine production in the colon.

Results—NCK2025 enhanced IL-10 production by dendritic cells and macrophages. Increased numbers of regulatory dendritic cells coincided with the induction of activated $FoxP3^+$ Tregs.

Conclusion—These results suggest that the oral administration of the genetically modified strain NCK2025 may be an effective immunotherapeutic approach that reprograms the immune response in colonic inflammatory conditions.

Keywords

dendritic cells; *Lactobacillus acidophilus*; macrophages; regulatory innate immune cells; Tregs

Discriminating antigen-recognition and -response mechanisms must be employed by the intestinal immune system in order to protect against potential pathogens, regulate inflammation and induce oral tolerance [1]. A better understanding of the immune mechanisms that underlie intestinal homeostasis may facilitate the development of new

*Author for correspondence: Tel.: +1 352 294 4117, Fax: +1 352 392 9704, m.zadeh@ufl.edu.

Ethical conduct of research

The authors state that they have obtained appropriate institutional review board approval or have followed the principles outlined in the Declaration of Helsinki for all human or animal experimental investigations. In addition, for investigations involving human subjects, informed consent has been obtained from the participants involved.

Financial & competing interests disclosure

This work was supported in part by the by NIH Grant 1R01AI098833-01. We also thank J Winter for her generous support. The authors have no other relevant affiliations or financial involvement with any organization or entity with a financial interest in or financial conflict with the subject matter or materials discussed in the manuscript apart from those disclosed.
No writing assistance was utilized in the production of this manuscript.

therapeutic approaches for various chronic inflammatory conditions, including inflammatory bowel disease (IBD). Although the precise cellular and molecular mechanisms by which intestinal commensal bacteria and their products impact IBD have yet to be defined, data show that the main feature of IBD is exaggerated inflammation characterized by infiltrating pathogenic IFN-$\gamma^{+}CD4^{+}$ T cells [2–6]. These cells can be triggered by the proinflammatory cytokine IL-12, produced by activated intestinal dendritic cells (DCs) stimulated by resident gut bacteria [7–9]. Such DC–bacterial interactions significantly impact the commitment and/or maintenance of various $CD4^{+}$ T-cell subsets [10], including Tregs [11,12]. In this respect, intestinal DCs discern and discriminate between different types of microbes and their gene products, a property that enables these cells to direct controlled protective T-cell immunity against pathogens and disease. Furthermore, these cells program immune regulation by rebalancing exaggerated inflammation via the production of regulatory cytokines (i.e., IL-10) and the induction of IL-10-producing Tregs [13,14].

Such immune regulation can be orchestrated by various DC subtypes, including $CD103^{+}$ DCs [15]. Regulatory DCs can produce IL-10 or the enzyme indoleamine 2,3-dioxygenase [16–19], or function via ligands such as inducible T-cell costimulator ligand [18], cytotoxic T lymphocyte antigen-4 or programmed death ligand [20]. It has recently been reported that the frequency of regulatory DCs is significantly increased upon infection with pathogens [21,22], including the causative agent of malaria [23]. These observations suggest that induced protective immunity against pathogens must be regulated in order to limit collateral damage caused by overt inflammation in the tissues. In the present study, we further clarify the cellular immune regulation orchestrated by the lipoteichoic acid (LTA)-deficient *Lactobacillus acidophilus* strain, NCK2025, in the normal steady state and in colitis caused by pathogenic $CD4^{+}$ T-cell transfer in *Rag1*$^{-/-}$ mice to highlight the genetically modified commensal bacterium's impact on intestinal immune cells and its potential role in immune therapeutic approaches.

Material & methods

Mice & reagents

C57BL/6 male and female breeders and C57BL/6 *Rag1*$^{-/-}$ mice were purchased from Jackson Laboratories (Bar Harbor, ME, USA). Mice were maintained in microisolator cages under specific pathogen-free, *Helicobacter*-free conditions. Sex- and age-matched mice were utilized in experiments performed according to NIH guidelines in the Guide for Care and Use of Laboratory Animals (NIH-72-23) and animal protocols approved by the local ethics committee.

Lactobacillus acidophilus NCFM strains

Wild-type *L. acidophilus* (NCK56) or LTA-deficient *L. acidophilus* (NCK2025) were propagated in de Man, Rogosa and Sharpe (MRS) broth (Difco™, BD Diagnostics, NJ, USA) at 37°C for 15 h. In preparation for oral treatment or *in vitro* stimulation, bacteria were

washed twice with sterile phosphate buffered saline (PBS) and the number of CFU of *L. acidophilus* strains were estimated by measuring the optical density at 600 nm [24]. The concentration of each *L. acidophilus* strain was adjusted to 1×10^{9} CFU/ml based on OD600 readings that had previously been correlated with CFU numbers [24]. Each mouse was orally treated with 5×10^{8} CFU bacterial strain; therefore 500 μl of 1×10^{9} CFU/ml suspension was centrifuged, pelleted and then resuspended in 100 μl of PBS. Each mouse was then treated with 100 μl PBS (control group) or 5×10^{8} CFU (of either *L. acidophilus* strain) orally in 100 μl sterile PBS. In some experiments, in order to determine the

persistence of erythromycin-resistant (Em^r) *L. acidophilus* strains, groups of mice were orally treated with 5×10^8 CFU/100 μl per mouse (n = 3). After 24 h, fecal pellets were collected from before, during and for up to 8 days after *L. acidophilus* oral treatments. Each fecal pellet (0.2 g/2 ml) was then dissolved in 10% MRS. The homogenized materials were serially diluted and plated onto MRS agar-containing Em^r (2 μg/ml). The daily average CFUs of either *L. acidophilus* strain in mouse feces were determined.

Immunofluorescence

NCK56 and NCK2025 cells were washed twice with sterile PBS and then labeled with AlexaFluor 647 (Invitrogen, CA, USA) in 0.1 M sodium bicarbonate buffer solution for 1 h at room temperature. Labeled bacteria cells were washed with PBS and resuspended with 0.1 M sodium bicarbonate at a concentration of 1×10^9 labeled bacteria per 100 μl of sodium bicarbonate. C57BL/6 mice were orally treated with 1×10^9 cells of AlexaFluor 647 NCK56 or AlexaFluor 647 NCK2025 cells. Mice were sacrificed 3 and 16 h later, and their colons were removed and prepared for immunofluorescence. Colons were filleted open, rolled, and snap frozen at −80°C in Tissue-Tek® OCT™ compound (Sakura, CA, USA); 5-μm sections were cut, fixed in ice-cold methanol (−20°C) for 15 min and blocked with 1% bovine serum albumin. For four-color immunostaining, sections were incubated overnight at 4°C with purified hamster anti-mouse CD11c (BD Biosciences, CA, USA) or biotin antimouse F4/80 (Biolegend, CA, USA) and rat antimouse IL-10 (Biolegend), followed by two washes with PBS and incubation with antihamster AlexaFluor 594 or streptavidin AlexaFluor 594 and antirat AlexaFluor 488 (Invitrogen) for 1 h. Sections were then washed twice with PBS, incubated for 10 min with 4,6-diamidino-2-phenylindole dihydrochloride (DAPI; Invitrogen), washed twice with PBS and mounted with antifade mounting medium as described previously [25]. Images were acquired using UV laser scanning microscopy confocal microscopy.

For three-color immunostaining, tissues were processed for frozen sectioning and staining as described above. The antibody combination used included biotin antimouse F4/80 (Biolegend), hamster antimouse CD11c (BD Biosciences), mouse antimouse CD4 (Abcam, MA, USA), rat antimouse FoxP3 (eBioscience, CA, USA), rat antimouse CD103, rat antimouse IL-10, rat anti-mouse IFN-γ, rat antimouse IL-12 and rat anti-mouse TNF-α (Biolegend). Images were acquired using TissueGnostics® (Vienna, Austria) Tissue/Cell High Throughput Imaging and Analysis System and analyzed using ImageJ software.

Pathogenic T-cell induced colitis

AffiniPure™ Goat Antimouse IgG (heavy and light chain-specific) purchased from Jackson ImmunoResearch Laboratories was used (at a final concentration of 100 mg/ml) to coat 5-ml Petri dishes overnight. The next day, the spleens were mechanically digested and red blood cells lysed with ammonium–chloride–potassium lysis buffer (Invitrogen). Splenocytes were then resuspended, transferred into IgG-coated Petri dishes and incubated at 37°C in supplemented complete RPMI-1640 medium. One dish was used for each spleen. All B lymphocytes, DCs and macrophages bound to the IgG coating on the surface of the Petri dish, while T lymphocytes remained in the media. An hour later, the media from the Petri dishes was collected into 50-ml conical tubes, washed with complete RPMI and counted. CD4 and CD25 isolation kits (Miltenyi Biotec, MA, USA) were utilized to enrich for $CD4^+CD25^-CD45Rb^{hi}$ T cells and for $CD4^+CD25^+$ T cells. At days 0 and 7, $CD4^+CD25^-CD45RB^{hi}$ T cells (10^6/100 μl PBS per mouse) were transferred to three groups of mice by intraperitoneal injection. A group of mice received $CD4^+CD25^-CD45RB^{hi}$ and $CD4^+CD25^+CD45RB^{low}$ Tregs on day 0 and 7 and served as a positive control group [26]. The day of the second injection of $CD4^+CD25^-CD45RB^{hi}$ T cells, the two groups of mice that received these pathogenic $CD4^+$ T cells were then given oral treatment with either

NCK56 or NCK2025 for 4 consecutive days. These mice were then treated once a week with NCK56 or NCK2025 for the next 4 weeks, and sacrificed after the last treatment. Additionally, a control mouse group receiving $CD4^+CD25^-CD45RB^{hi}$ T cells alone without bacterial treatment was also utilized to demonstrate unsuppressed colitis induction. Control mice groups received oral treatment with 100 μl of PBS per mouse during the times that the other two groups were treated with either NCK56 or NCK2025.

Statistics

Statistics were performed using Microsoft Prism. One-way ANOVA was performed to analyze statistical significance of the data. $p \leq 0.05$ indicates statistical significance between the study groups.

Results

Enhancement of regulatory innate cells by NCK2025

Adaptation of regulatory innate immune cells, including DCs, to the intestinal environment is crucial for the prevention of destructive inflammatory responses [27]. Even though intestinal DCs are involved in the induction of active immune responses aimed at controlling the normal intestinal flora [28], these cells may also induce tolerogenic responses towards gut commensals by activating regulatory immune mechanisms. During steady-state conditions, intestinal DCs with regulatory potential migrate towards the lymph nodes after sampling antigens in the intestinal tissues [29]. After migrating towards the mesenteric lymph nodes, DCs interact with T cells to initiate responses that are aimed at maintaining a noninflammatory environment in the intestines [29]. To further elucidate the regulatory potential of LTA-deficient NCK2025 and its impact on innate and adaptive immunity in both steady-state and disease conditions, we first orally administered Em^r-resistant NCK56 and NCK2025 to demonstrate the ability of these bacterial strains to colonize the gut. As seen in Figure 1A, mice were able to clear both NCK56 and NCK2025 after day 3, with slightly less NCK2025 excreted on days 2 and 3. To demonstrate transient colonization of the gut by these strains, mice were treated with the same bacterial strains 1 week later. Once again, data indicate that these strains can be detected in the feces of the animals and that the colonization of these strains is clearly transient (Figure 1A). Moreover, deletion of the phosphoglycerol transferase enzyme, which is responsible for LTA expression on the surface of NCK2025, does not impair the survival of this strain in the gut. These studies were essential in determining the time of bacterial clearance from the gut in order to delineate the time kinetics utilized in the present studies.

IL-10 posess numerous suppressive functions involved in dampening inflammatory responses, including inhibition of myeloid cell maturation and reduction in the expression of costimulatory molecules on DCs [30]. Thus, we analyzed the ability of $CD11c^+$ DCs and $F4/80^+$ macrophages to produce IL-10 in the colons of bacteria-treated mice after capturing AlexaFluor 647-labeled NCK56 and NCK2025, compared with PBS-treated control mice. Confocal microscopy analyses showed that $CD11c^+$ DCs and $F4/80^+$ macrophages located in the colonic tissue captured labeled bacteria and produced IL-10 (Figure 1B). We then quantified producers of IL-10 upon bacteria capture using high-throughput imaging. Interestingly, there was a delay in IL-10 production by $CD11c^+$DCs capturing NCK2025; the peak of IL-10 production in response to NCK56 was at 3 h, but was at 16 h for NCK2025 (Figure 1C). Even though there is an elevation in IL-10 production by NCK56-capturing $F4/80^+$macrophages at 3 h, the peak production of IL-10 by macrophages in response to both NCK56 and NCK2025 is attained at 16 h (Figure 1D). At this 16 h time point, significantly more IL-10 was produced by macrophages in response to NCK2025 than to NCK56 (Figure 1D). These data may suggest that a secondary less-efficient recognition

mechanism exists, perhaps utilizing one of the other surface layer proteins present on NCK2025.

Since initial results indicated that treatment with NCK2025 induces regulatory DCs [17,31], fluorescent microscopy was employed to examine cell populations in the colon in order to avoid any undesired cell death caused by harmful enzymatic reagents necessary for cell isolation. In the colons of PBS- and bacteria-treated mice at day 1 and 3 following bacterial treatment, a significantly higher percentage of $CD11c^+$ cells per total $DAPI^+$ cells produced IL-10 in NCK2025-treated mice compared with PBS- or NCK56-treated mice (Figure 2A). These differences in IL-10 production by DCs were absent at day 7 in the colons (Figure 2A). At the same time points of days 1 and 3, a significantly greater percentage of $CD11c^+$ cells per total $DAPI^+$ cells released TNF-α (Figure 2B) and IL-12 (Figure 2C) in the colons of NCK56-treated mice compared with the colons of NCK2025- and PBS-treated mice. However, by day 7, the frequencies of TNF-α- and IL-12-producing $CD11c^+$ cells normalized to the levels of PBS- and NCK2025-treated mice (Figure 2B & C).

In order to study the role of macrophages in the immune response elicited against NCK56 and NCK2025, the production of IL-10 by $F4/80^+$ cells was also evaluated (Figure 2D). By day 1 following bacteria treatment, a significantly greater percentage of colonic $F4/80^+$cells from NCK2025-treated mice produced IL-10 when compared with NCK56- or PBS-treated mice (Figure 2D). IL-10 production by $F4/80^+$ cells decreased by day 3 in mice that were treated with both bacterial strains, and the IL-10 production levels were reduced to the baseline of PBS-treated mice by day 7 using both strain treatments (Figure 2D). These data suggest that the molecular properties of bacterial stimuli play an important role in the stimulation of colonic DCs and macrophages, which may then determine the outcome of the intestinal immunity.

Previously, we have established the critical role of functional $FoxP3^+$ T cells in experimental colitis and showed how these cells can be induced by regulatory $IL\text{-}10^+$ DCs [17]. In this report, we demonstrate the induction of colonic Tregs in mice treated with PBS, NCK56 or NCK2025. Data show that oral NCK2025 treatment significantly enhanced the generation of $FoxP3^+IL\text{-}10^+$ Tregs within the colon after day 1 when compared with NCK56- or PBS-treated mice (Figure 3A). Interestingly, after days 3 and 7, the frequencies of these cells were normalized to the levels of PBS-treated mice (Figure 3A). In addition, $CD4^+IL\text{-}10^+$ T cells (Figure 3B) and $CD4^+IFN\text{-}\gamma^+$ T cells (Figure 3C) were investigated by high-throughput imaging TissueGnostics (TissueGnostics GmbH). As seen in Figure 3B, $CD4^+IL\text{-}10^+$ T cells were present in high numbers within the colonic tissues of NCK2025-treated mice within day 1. After days 3 and 7, the frequencies of these cells were downregulated in all groups (Figure 3B). Moreover, the release of IFN-γ by $CD4^+$ T cells indicates that NCK56 upregulates the production of this cytokine in colonic $CD4^+$ T cells when compared with NCK2025- or PBS-treated mice (Figure 3C). The production of IFN-γ by these $CD4^+$ T cells may play a detrimental role in the progression of IBD [2].

Regulation of colonic immunity in *Rag1*$^{-/-}$ by NCK2025

Previously, we demonstrated that NCK2025 ameliorates pathogenic $CD4^+CD45^{hi}$ T-cell-induced colitis in *Rag1*$^{-/-}$ mice [17]. In order to elucidate the immune mechanisms by which the NCK2025 strain dampens inflammation *in vivo*, pathogenic $CD4^+CD25^-CD45RB^{hi}$ T cells were transferred via intraperitoneal injection into *Rag1*$^{-/-}$ mice on days 0 and 7. Beginning on the day of the last pathogenic T-cell injection, three groups of mice were treated orally with PBS, NCK56 or NCK2025 for 4 consecutive days, and then once a week for the next 4 weeks. One group of mice received $CD4^+CD25^-CD45RB^{hi}$ (pathogenic $CD4^+$ T cells) and $CD4^+CD25^+CD45RB^{low}$ (Tregs) T cells, acting as a positive control group. In conjunction with previously published data, our

data indicate that *Rag1*$^{-/-}$ mice injected with pathogenic CD4^{+}T cells with or without oral NCK56 treatment developed colitis. Mice injected with the pathogenic T cells and given NCK2025 had a lower disease activity index (DAI) and did not lose as much weight as mice that received NCK56 or PBS (data not shown) [17]. As expected, mice that received pathogenic CD4^{+} T cells and Tregs did not develop colitis, as determined by a lack of weightloss and a DAI of zero (data not shown). Furthermore, histological analyses revealed that the colons of *Rag1*$^{-/-}$ mice 44 days following pathogenic T-cell transfer exhibited ongoing colitis and ulceration; whereas the colons of mice treated with NCK2025 in addition to the pathogenic T-cell injections showed accelerated healing and regenerated intestinal crypt structures, with continued inflammation limited primarily to the mucosa (data not shown). NCK56 treatment very mildly improved histological colitis scores with restitution of the epithelium, but also showed limited crypt regeneration and ongoing active inflammation within the mucosa (data not shown) [17].

In order to evaluate the cellular mechanisms involved in pathogenic CD4^{+} T-cell-mediated colitis and its regulation by NCK2025 treatment, we employed fluorescent microscopy. Data show that CD11c^{+}CD103^{+}IL-10^{+} cells were present in all groups of mice. However, these cells also produced high levels of TNF-α and IL-12 in mice that received pathogenic CD4^{+} T cells along with PBS or NCK56 treatment (Figure 4A & B). By contrast, CD11c^{+}IL-10^{+} DCs in mice treated with pathogenic CD4^{+} T cells with NCK2025 produced significantly less TNF-α or IL-12 (Figure 4A & B). Recently, it has been shown that mesenteric lymph node-derived CD103^{+} DCs isolated from mice with colitis had an impaired ability to induce FoxP3^{+} Tregs. Conversely, these cells had an enhanced ability to prime proinflammatory CD4^{+} IFN-γ-secreting cells [32]. As seen in Figures 5 & 6, although CD11c^{+}IL-10^{+}, F4/80^{+}IL-10^{+}, CD4^{+}IL-10^{+} and CD11c^{+}CD103^{+} cells are present in the groups of mice that received CD4^{+}CD45RB^{hi} T cells (pathogenic CD4^{+} T cells) with PBS or NCK56 treatment, elevated levels of CD4^{+}IFN-γ^{+} T cells were also observed in these groups of mice (Figures 5 & 6). By contrast, *Rag1*$^{-/-}$ mice that received pathogenic CD4^{+} T cells with NCK2025 treatment showed a significant decrease in the levels of colonic CD4^{+}IFN-γ^{+} T cells, similar to what was seen in mice in which CD4^{+}CD45RB^{hi} T cells plus Tregs were transferred (Figures 5 & 6). These data highlight the role of the LTA-deficient strain, NCK2025, in the direction of immune regulation by well-balanced DCs that control colonic CD4^{+} T-cell function in *Rag1*$^{-/-}$ mice.

The frequency of CD4^{+} T cells in the colons of mice that received pathogenic CD4^{+} T cells along with PBS or NCK56 was higher than in NCK2025-treated mice (Figures 5 & 6). While the absolute levels of CD4^{+}FoxP3^{+} T cells were increased in the groups of mice receiving pathogenic CD4^{+} T cells with PBS or NCK56 compared with treatment with NCK2025, this reduction in the CD4^{+} and CD4^{+}FoxP3^{+} T-cell levels in NCK2025-treated animals could be attributable to the very low DAI score of NCK2025-treated mice. Moreover, the trend of an increased total FoxP3^{+}:CD4^{+}-T cell ratio was seen in *Rag1*$^{-/-}$ mice that were treated with pathogenic CD4^{+} T cells with NCK2025 (Figure 6) when compared with mice receiving pathogenic CD4^{+} T cells along with PBS or NCK56. A significantly higher CD4^{+} and CD4^{+}FoxP3^{+} T-cell population and FoxP3^{+}:CD4^{+} T-cell ratio was also seen in Treg-treated control mice due to the adoptive transfer of Tregs. This indicates that CD4^{+} T cells may be tightly regulated by FoxP3^{+} Tregs that were induced by regulatory IL-10^{+}CD103^{+} DCs during the disease course, a unique property described for intestinal CD103^{+} DCs that regulate mucosal immunity, immune homeostasis and imprint gut homing phenotypic changes of T-cell subsets [33].

These findings indicate that LTA deficiency in NCK2025 enables this genetically modified strain to deliver regulatory signals to innate immune cells (i.e., DCs), which in turn elicit the induction of colonic immune regulation, resulting in the amelioration of both disease

progression and inflammation. The development of this unique commensal bacteria strain presents a novel opportunity to develop therapies that can safely modulate and reprogram inflammation *in vivo*. Ongoing studies in our laboratory will further dissect the critical molecules expressed on the surface of this bacterium in the normal steady state and during induced inflammation *in vivo*.

Conclusion & future perspective

Recently, significant progress in the understanding of the cellular and molecular pathogeneses of IBD has been achieved using murine models for ulcerative colitis, highlighting the critical role of commensal microbiota and their gene products in the immunopathology of IBD [4]. Data show that deregulation of immune interactions that promote intestinal homeostasis leads to cellular immune dysfunctions, which may result in undesired intestinal inflammation and IBD progression. The precise cellular and molecular mechanisms of IBD remain poorly understood. Questions remain as to how intestinal inflammatory immune components become proinflammatory, and how they can be reprogrammed. In this regard, we have recently demonstrated a pivotal role for gut microflora (i.e., *L. acidophilus* NCFM) in controlling inflammation of the intestine.

Collectively, our data indicate that the LTA-deficient strain, NCK2025, activates DC and macrophage regulation, which in turn directly elicits $CD4^+$ Treg activation. Furthermore, we demonstrate that stimulatory bacterial gene products (i.e., LTA) modify innate and adaptive immune responses *in vivo*. Such an activation of $CD4^+$ effector T cells may result in the promotion of chronic inflammation in IBD [34]. Studies are currently underway to further modify the gene products of *L. acidophilus* in order to investigate whether dysregulated immune functions can be restored using gene targeting to mitigate colonic diseases, including IBD and colon cancer.

References

1. Mowat AM. Anatomical basis of tolerance and immunity to intestinal antigens. Nat Rev Immunol. 2003; 3(4):331–341. [PubMed: 12669023]
2. MacDonald TT, Gordon JN. Bacterial regulation of intestinal immune responses. Gastroenterol Clin North Am. 2005; 34(3):401–412. VII–VIII. [PubMed: 16084304]
3. Neurath MF, Fuss I, Kelsall BL, et al. Experimental granulomatous colitis in mice is abrogated by induction of TGF-β-mediated oral tolerance. J Exp Med. 1996; 183(6):2605–2616. [PubMed: 8676081]
4. Xavier RJ, Podolsky DK. Unravelling the pathogenesis of inflammatory bowel disease. Nature. 2007; 448(7152):427–434. [PubMed: 17653185]
5. Baumgart DC, Carding SR. Inflammatory bowel disease: cause and immunobiology. Lancet. 2007; 369(9573):1627–1640. [PubMed: 17499605]
6. Baumgart DC, Sandborn WJ. Inflammatory bowel disease: clinical aspects and established and evolving therapies. Lancet. 2007; 369(9573):1641–1657. [PubMed: 17499606]
7. Powrie F. T cells in inflammatory bowel disease: protective and pathogenic roles. Immunity. 1995; 3(2):171–174. [PubMed: 7648390]
8. Cheroutre H. In IBD eight can come before four. Gastroenterology. 2006; 131(2):667–670. [PubMed: 16890619]
9. Elson CO, Cong Y, McCracken VJ, et al. Experimental models of inflammatory bowel disease reveal innate, adaptive, and regulatory mechanisms of host dialogue with the microbiota. Immunol Rev. 2005; 206:260–276. [PubMed: 16048554]
10. Ivanov II, Atarashi K, Manel N, et al. Induction of intestinal Th17 cells by segmented filamentous bacteria. Cell. 2009; 139(3):485–498. [PubMed: 19836068]

11. Mazmanian SK, Kasper DL. The love–hate relationship between bacterial polysaccharides and the host immune system. Nat Rev Immunol. 2006; 6(11):849–858. [PubMed: 17024229]
12. Mazmanian SK, Liu CH, Tzianabos AO, Kasper DL. An immunomodulatory molecule of symbiotic bacteria directs maturation of the host immune system. Cell. 2005; 122(1):107–118. [PubMed: 16009137]
13. Belkaid Y, Oldenhove G. Tuning microenvironments: induction of regulatory T cells by dendritic cells. Immunity. 2008; 29(3):362–371. [PubMed: 18799144]
14. Morelli AE, Thomson AW. Tolerogenic dendritic cells and the quest for transplant tolerance. Nat Rev Immunol. 2007; 7(8):610–621. [PubMed: 17627284]
15. Coombes JL, Siddiqui KR, Arancibia-Carcamo CV, et al. A functionally specialized population of mucosal $CD103^+$ DCs induces $FoxP3^+$ regulatory T cells via a TGF-β and retinoic acid-dependent mechanism. J Exp Med. 2007; 204(8):1757–1764. [PubMed: 17620361]
16. Akbari O, DeKruyff RH, Umetsu DT. Pulmonary dendritic cells producing IL-10 mediate tolerance induced by respiratory exposure to antigen. Nat Immunol. 2001; 2(8):725–731. [PubMed: 11477409]
17. Mohamadzadeh M, Pfeiler EA, Brown JB, et al. Regulation of induced colonic inflammation by *Lactobacillus acidophilus* deficient in lipoteichoic acid. Proc Natl Acad Sci USA. 2011; 108(Suppl 1):S4623–S4630.
18. Ito T, Yang M, Wang YH, et al. Plasmacytoid dendritic cells prime IL-10-producing T regulatory cells by inducible costimulator ligand. J Exp Med. 2007; 204(1):105–115. [PubMed: 17200410]
19. Sharma MD, Baban B, Chandler P, et al. Plasmacytoid dendritic cells from mouse tumor-draining lymph nodes directly activate mature Tregs via indoleamine 2,3-dioxygenase. J Clin Invest. 2007; 117(9):2570–2582. [PubMed: 17710230]
20. Probst HC, McCoy K, Okazaki T, Honjo T, van den Broek M. Resting dendritic cells induce peripheral $CD8^+$ T cell tolerance through PD-1 and CTLA-4. Nat Immunol. 2005; 6(3):280–286. [PubMed: 15685176]
21. Probst HC, van den Broek M. Priming of CTLs by lymphocytic choriomeningitis virus depends on dendritic cells. J Immunol. 2005; 174(7):3920–3924. [PubMed: 15778347]
22. Bonifazi P, Zelante T, D'Angelo C, et al. Balancing inflammation and tolerance *in vivo* through dendritic cells by the commensal *Candida albicans*. Mucosal Immunol. 2009; 2(4):362–374. [PubMed: 19421183]
23. Wong KA, Rodriguez A. *Plasmodium* infection and endotoxic shock induce the expansion of regulatory dendritic cells. J Immunol. 2008; 180(2):716–726. [PubMed: 18178809]
24. Carrol IM, Andrus JM, Bruno-Bárcena JM, et al. Anti-inflammatory properties of *Lactobacillus gasseri* expressing manganese superoxide dismutase using the interleukin 10-deficient mouse model of colitis. Am J Physiol Gastrointest Liver Physiol. 2007; 293:729–738.
25. Gounaris E, Tung CH, Restaino C, et al. Live imaging of cysteine–cathepsin activity reveals dynamics of focal inflammation, angiogenesis, and polyp growth. PLoS ONE. 2008; 3(8):E2916. [PubMed: 18698347]
26. Murai M, Turovskaya O, Kim G, et al. Interleukin 10 acts on regulatory T cells to maintain expression of the transcription factor FoxP3 and suppressive function in mice with colitis. Nat Immunol. 2009; 10(11):1178–1184. [PubMed: 19783988]
27. Iliev ID, Mileti E, Matteoli G, Chieppa M, Rescigno M. Intestinal epithelial cells promote colitis-protective regulatory T-cell differentiation through dendritic cell conditioning. Mucosal Immunol. 2009; 2(4):340–350. [PubMed: 19387433]
28. Kelsall B. Recent progress in understanding the phenotype and function of intestinal dendritic cells and macrophages. Mucosal Immunol. 2008; 1(6):460–469. [PubMed: 19079213]
29. Schulz O, Jaensson E, Persson EK, et al. Intestinal $CD103^+$, but not $CX3CR1^+$, antigen sampling cells migrate in lymph and serve classical dendritic cell functions. J Exp Med. 2009; 206(13): 3101–3114. [PubMed: 20008524]
30. Moore KW, de Waal Malefyt R, Coffman RL, O'Garra A. Interleukin-10 and the interleukin-10 receptor. Ann Rev Immunol. 2001; 19:683–765. [PubMed: 11244051]
31. Saber R, Zadeh M, Pakanati KC, et al. Lipoteichoic acid-deficient *Lactobacillus acidophilus* regulates downstream signals. Immunotherapy. 2011; 3(3):337–347. [PubMed: 21395377]

32. Laffont S, Siddiqui KR, Powrie F. Intestinal inflammation abrogates the tolerogenic properties of MLN CD103^{+} dendritic cells. Eur J Immunol. 2010; 40(7):1877–1883. [PubMed: 20432234]

33. Bogunovic M, Ginhoux F, Helft J, et al. Origin of the lamina propria dendritic cell network. Immunity. 2009; 31(3):513–525. [PubMed: 19733489]

34. Waldner MJ, Neurath MF. Cytokines in colitis associated cancer: potential drug targets? Inflamm Allergy Drug Targets. 2008; 7(3):187–194. [PubMed: 18782026]

Executive summary

- Ulcerative colitis and Crohn's disease are thought to be induced by exaggerated inflammation, often characterized as inflammatory bowel disease.
- Pathogenic $CD4^+$ T cells play a critical role in gut inflammation and tissue destruction when induced by peripherally activated dendritic cells that recognize bacterial gene products.
- Lipoteichoic acid is an amphiphilic, negatively charged glycolipid that facilitates bacterial adhesion, colonization and invasion.
- Lipoteichoic acid shares many of the inflammatory properties of a lipopolysaccharide, and plays a role in the pathogenesis of septic shock or severe inflammatory responses induced by Gram-positive bacterial infection via pattern-recognition receptors, including Toll-like receptors.
- Tregs, best characterized by the transcription factor FoxP3, play a critical role in maintaining self-tolerance.
- Tregs modulate the host immune response in inflammation and infectious diseases, and are key players of peripheral tolerance.

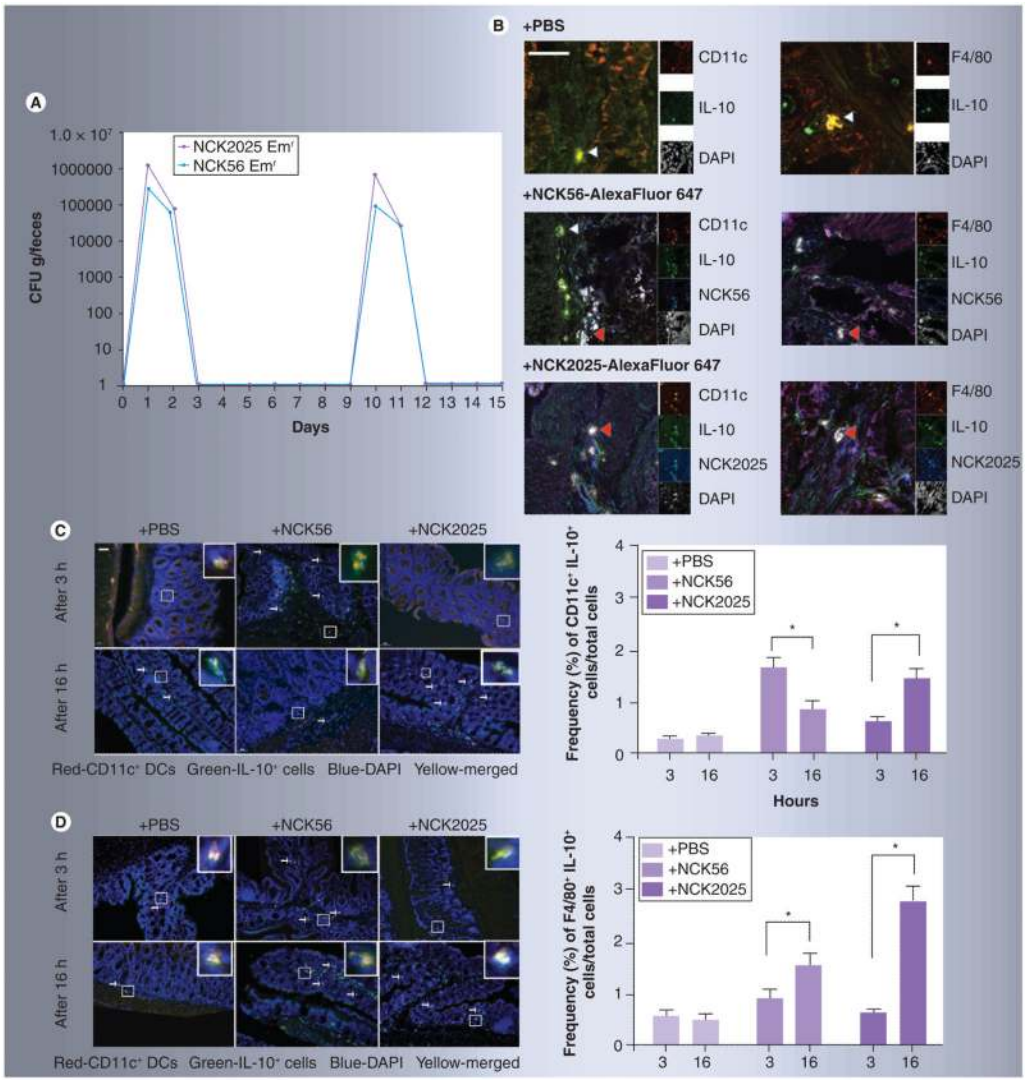

Figure 1. Transient colonization of the gut and bacterial uptake by colonic dendritic cells and macrophages

(A) Groups of mice (n = 3) were orally treated with Em^r NCK56 or NCK2025 cells (5×10^8 CFU/100 µl per mouse). Fecal pellets were collected before, during and for up to 8 days after bacterial oral treatments, and dissolved in 10% de Man, Rogosa and Sharpe broth (MRS). The homogenized materials were serially diluted and plated onto MRS agar containing erythromycin (2 µg/ml). The daily average number of CFU of either *Lactobacillus acidophilus* strain in mouse feces was determined. Data are representative of at least three independent experiments. **(B)** Confocal microscopy images of colons from mice treated with PBS and NCK56 or NCK2025 cells. NCK56 or NCK2025 cells were labeled with AlexaFluor 647 (blue). 5-µm sections were stained with an anti-IL-10 antibody (green), and for DCs (anti-CD11c, red) or macrophages (anti-F4/80, red). Magnification ×630 (white scale bar represents 50 µm). The main images are the merge of three channels (red, green and blue). The double-positive cells are yellow (indicated by white arrowheads) and the triple-positive cells are white (indicated by red arrowheads). On the right of the main images are thumbnails of the single-color images, as well as the DAPI image in gray. **(C & D)** AlexaFluor 647-labeled NCK56- or NCK2025-treated and untreated (PBS) mouse colons were stained with CD11c or F4/80 (red cells) and IL-10 (green cells) antibodies and

visualized by TissueGnostics® Tissue/Cell High-Throughput Imaging and Analysis System. **(C)** Representation and quantification of IL-10 production by $CD11c^+$ DCs at 3 and 16 h following PBS, NCK56 or NCK2025 treatment. **(D)** Representation and quantification of IL-10 production by $F4/80^+$ macrophages at 3 and 16 h following PBS, NCK56 or NCK2025 treatment. Data were statistically analyzed by one-way ANOVA.
$^*p < 0.05$ indicates significance of the data between the study groups.
DAPI: 4,6-diamidino-2-phenylindole dihydrochloride; DC: Dendritic cell; Em^r: Erythromycin resistant; PBS: Phosphate buffered saline.

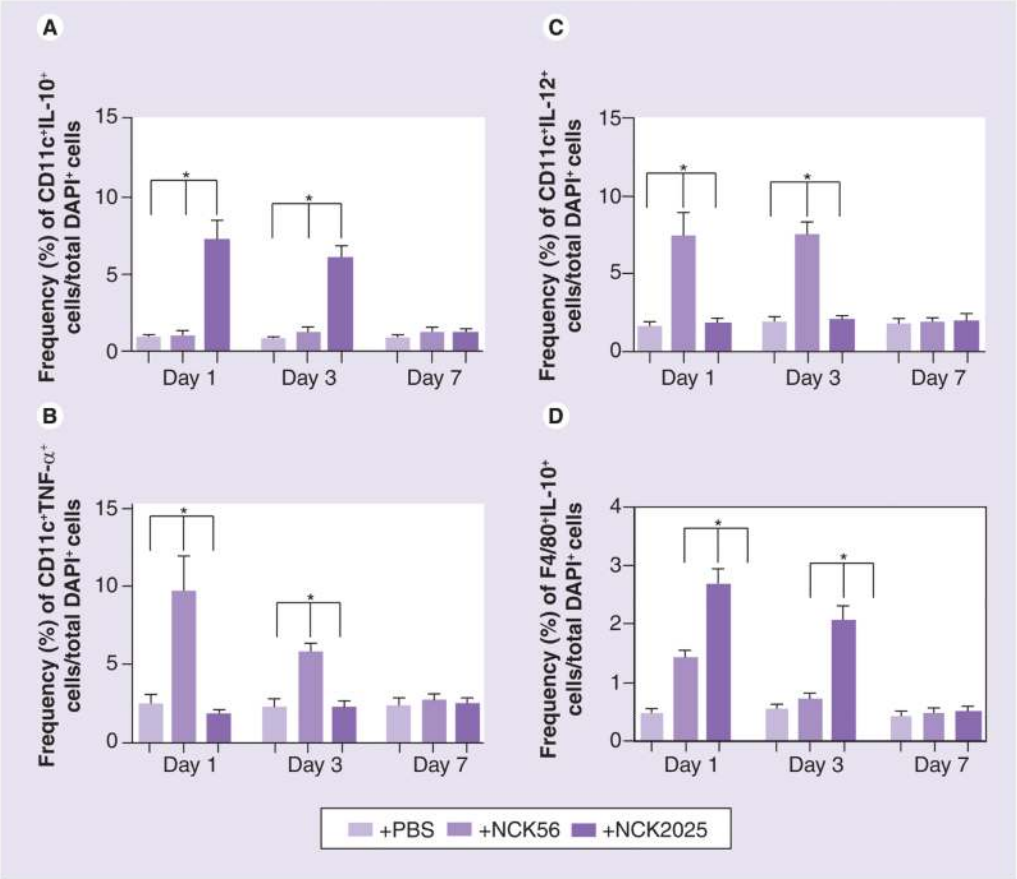

Figure 2. Regulation of colonic dendritic cells and macrophages by NCK2025 cells

(A–D) PBS-, NCK56- or NCK2025-treated mouse colons were stained with CD11c, F4/80, TNF-α, IL-12 or IL-10 antibodies and visualized by TissueGnostics® Tissue/Cell High-Throughput Imaging and Analysis System. This shows the quantification of the frequencies of **(A)** $CD11c^+IL\text{-}10^+$ dendritic cells (DCs), **(B)** $CD11c^+TNF\text{-}\alpha^+$ DCs, **(C)** $CD11c^+IL\text{-}12^+$ DCs and **(D)** $F4/80^+IL\text{-}10^+$ macrophages in the colons of mice treated with PBS, NCK56 or NCK2025 at days 1, 3 and 7. Data were statistically analyzed by one-way ANOVA.
*$p < 0.05$ indicates significance of the data between the study groups.
DAPI: 4,6-diamidino-2-phenylindole dihydrochloride; PBS: Phosphate buffered saline.

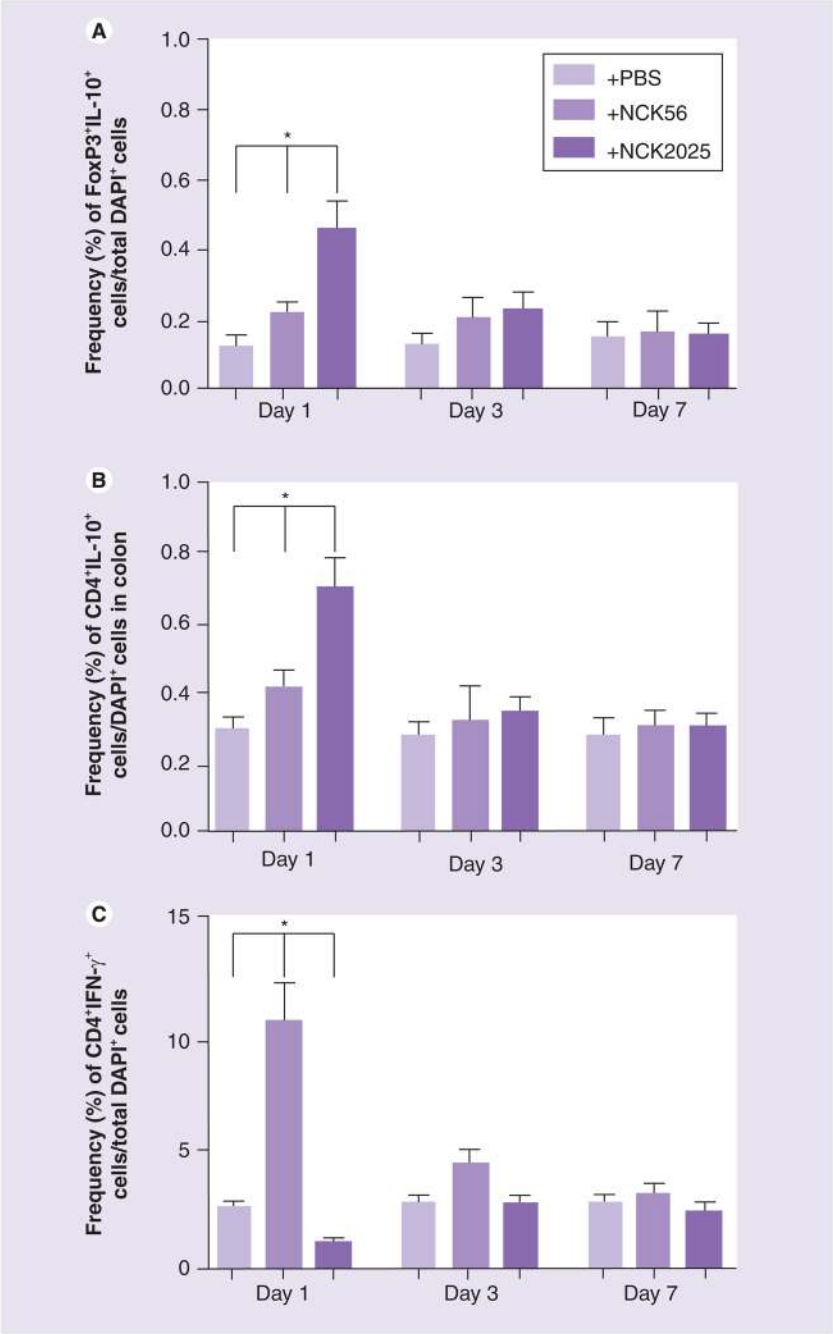

Figure 3. Regulation of colonic T cells by NCK2025

(A–C) PBS-, NCK56- or NCK2025-treated mouse colons were stained with CD4, FoxP3, IL-10 or IFN-γ antibodies and visualized by TissueGnostics® Tissue/Cell High-Throughput Imaging and Analysis System. Figure shows quantification of the frequencies of **(A)** $FoxP3^+IL\text{-}10^+$ T cells, **(B)** $CD4^+IL\text{-}10^+$ T cells and **(C)** $CD4^+IFN\text{-}\gamma^+$ T cells in the colons of mice treated with PBS, NCK56 or NCK2025 at days 1, 3, and 7. Data were statistically analyzed by one-way ANOVA.

*$p < 0.05$ indicates significance of the data between the study groups.

DAPI: 4,6-diamidino-2-phenylindole dihydrochloride; PBS: Phosphate buffered saline.

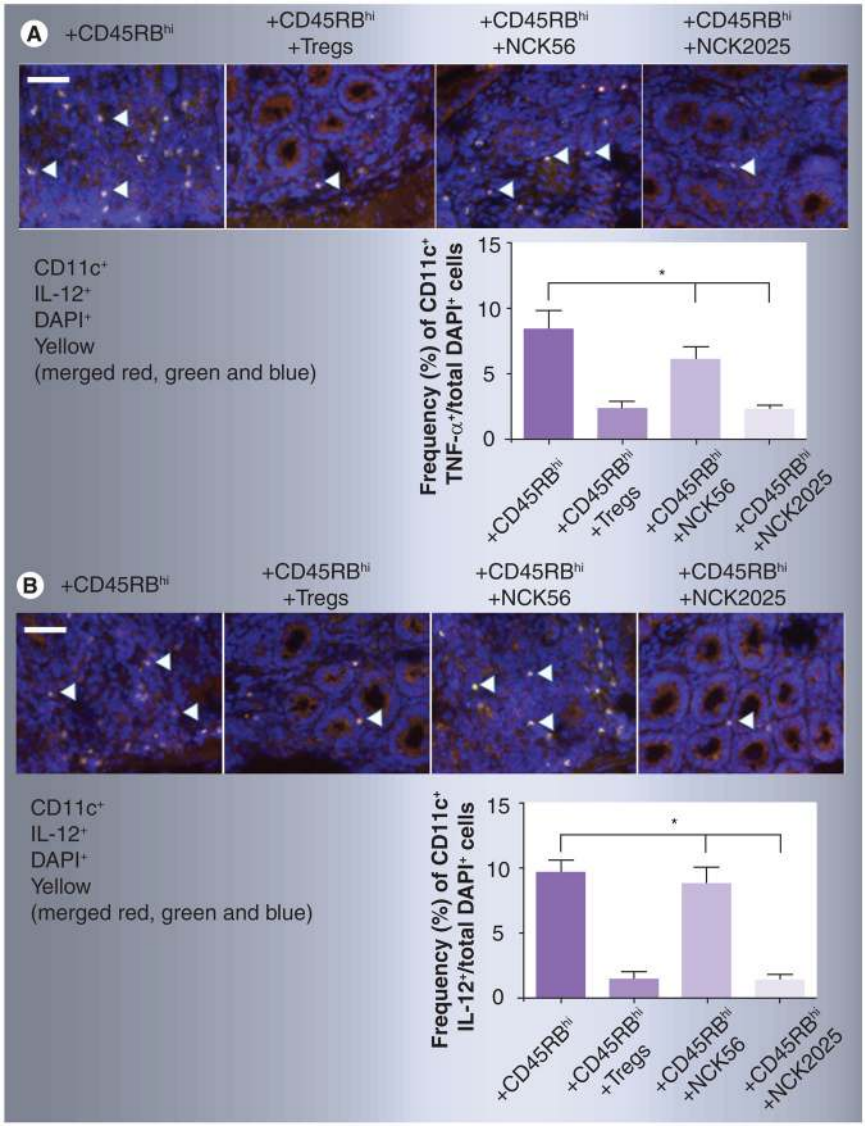

Figure 4. Regulation of pathogenic CD4$^+$CD45RB^{hi} T cells in *Rag1*$^{-/-}$ mice by NCK2025

(A & B) Colons from *Rag1*$^{-/-}$ mice receiving pathogenic CD4$^+$ T cells along with phosphate buffered saline, Tregs, NCK56 or NCK2025 treatment were stained with CD11c (red cells) antibodies and TNF-α or IL-12 (green cells) antibodies and visualized by TissueGnostics® Tissue/Cell High-Throughput Imaging and Analysis System. The figure shows the representation and quantification of **(A)** CD11c$^+$TNF-α$^+$ and **(B)** CD11c$^+$IL-12$^+$ dendritic cells. Data were statistically analyzed by one-way ANOVA.

*$p < 0.05$ indicates significance of the data between the study groups. White scale bar represents 50 μm. Colocalized double-positive cells are yellow, as indicated by white arrowheads.

DAPI: 4,6-diamidino-2-phenylindole dihydrochloride.

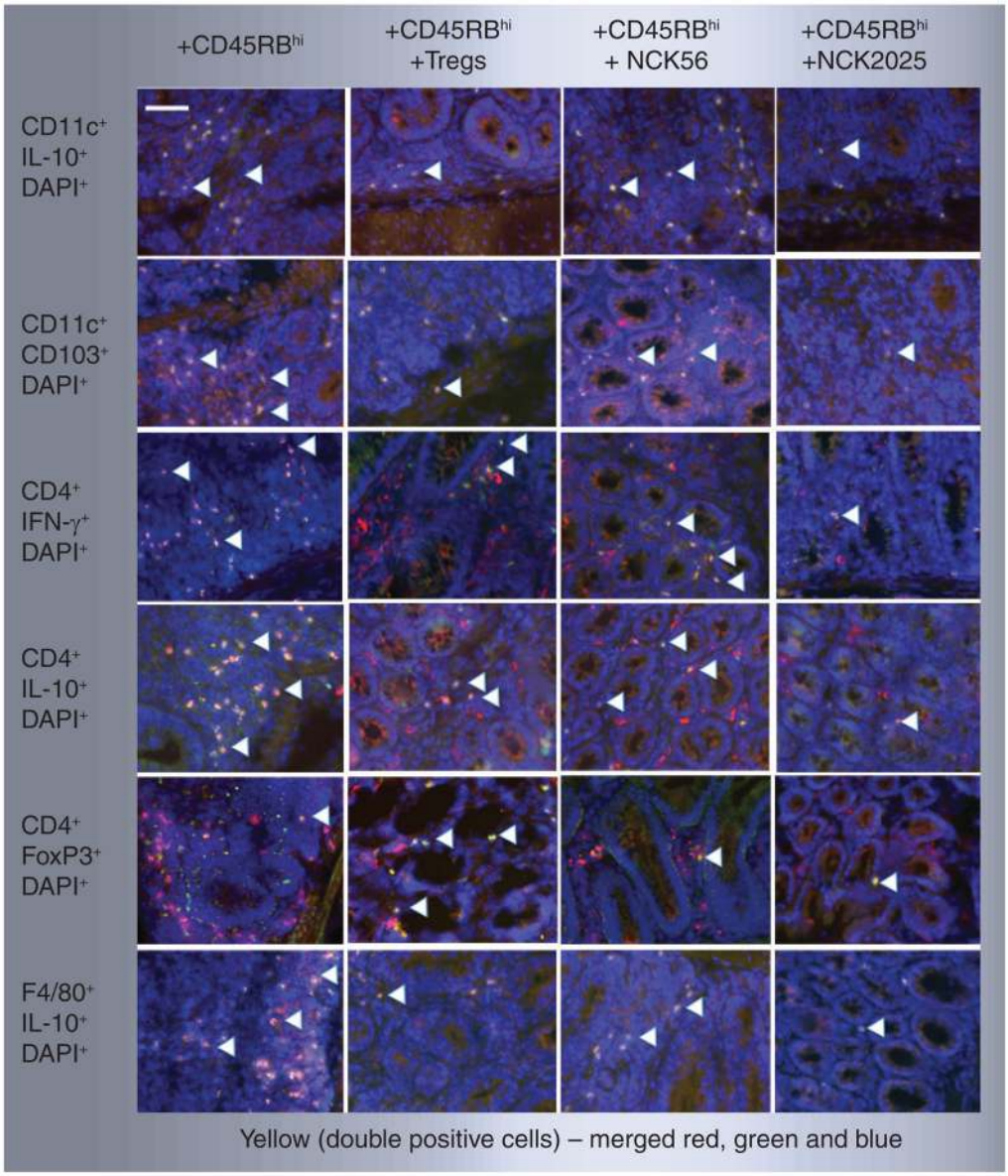

Figure 5. Immuneregulation of pathogenic CD4$^+$CD45RB^{hi} T cells by NCK2025

Colons from *Rag1*$^{-/-}$ mice receiving pathogenic CD4$^+$ T cells along with PBS, Tregs, NCK56 or NCK2025 treatment were stained with CD11c, CD4, F4/80 (red cells) antibodies, IL-10, CD103, IFN-γ or FoxP3 (green cells) antibodies and visualized by TissueGnostics® Tissue/Cell High-Throughput Imaging and Analysis System. The figure depicts representative pictures. The white scale bar represents 50 μm, colocalized double-positive cells are yellow indicated by white arrowheads. DAPI: 4,6-diamidino-2-phenylindole dihydrochloride.

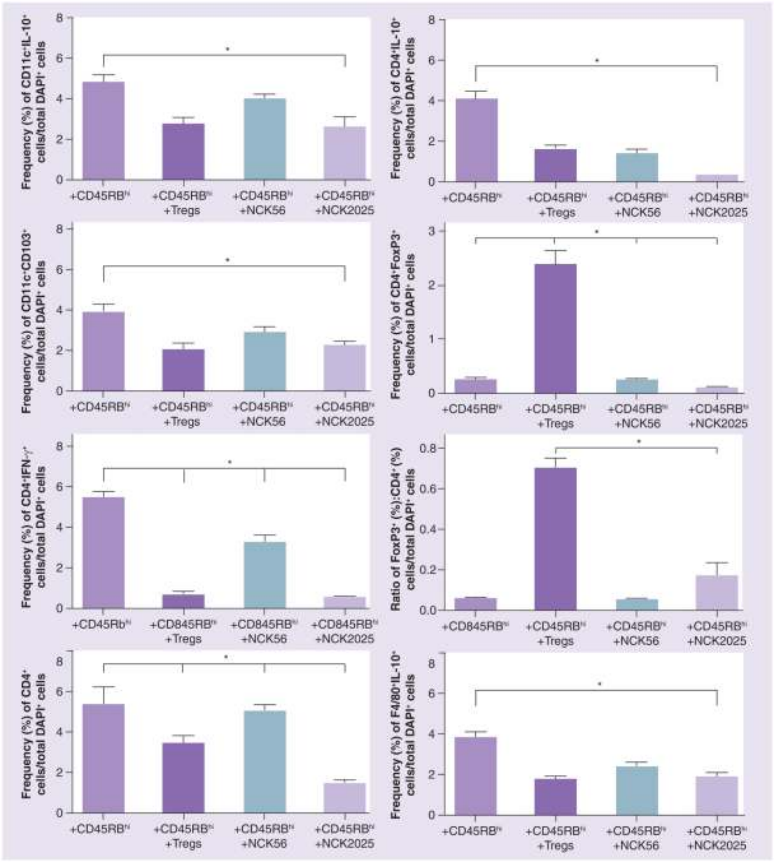

Figure 6. Regulation of pathogenic CD4$^+$CD45RB^{hi} T cells *in vivo* by NCK2025

Quantification of the frequencies of CD11c$^+$IL-10$^+$, CD11c$^+$CD103$^+$, CD4$^+$IFN-γ$^+$, CD4$^+$IL-10$^+$ and CD4$^+$FoxP3$^+$ cells; ratio (%) of Foxp3: CD4$^+$ T cells; and F4/80$^+$IL-10$^+$ cells in colons of *Rag1*$^{-/-}$ mice (n = 5/group) treated with phosphate buffered saline, NCK56 or NCK2025. Data were statistically analyzed by one-way ANOVA. *$p < 0.05$ indicates the significance of the data between the study groups.